OXFORD UNIVERSITY PRESS | Schizophrenia Bulletin



# Ketamine Dysregulates the Amplitude and Connectivity of High-Frequency Oscillations in Cortical-Subcortical Networks in Humans: Evidence from Resting-State MEG-Recordings



| | |
|---|---|
| Journal: | *Schizophrenia Bulletin* |
| Manuscript ID: | SZBLTN-ART-14-0390.R2 |
| Manuscript Type: | Regular Article |
| Date Submitted by the Author: | n/a |
| Complete List of Authors: | Rivolta, Davide; University of East London,<br>Heidegger, Tonio; Goethe-University, Clinical for Neurology<br>Scheller, Bertram; Goethe-University, Clinic for Anesthesia<br>Sauer, Andreas; MPI for Brain Research,<br>Schaum, Michael; Goethe University, MEG-Unit<br>Birkner, Katharina; MPI for Brain Research,<br>Singer, Wolf; MPI for Brain Research,<br>Wibral, Michael; Goethe-University, MEG-Unit<br>Uhlhaas, Peter; University of Glasgow, Institute of Neuroscience and Psychology |
| Keywords: | Ketamine, MEG, Oscillations |
| | |

# Ketamine Dysregulates the Amplitude and Connectivity of High-Frequency Oscillations in Cortical-Subcortical Networks in Humans: Evidence from Resting-State MEG-Recordings

Rivolta Davide[1,2,3], Ph.D., Heidegger Tonio[4], M.D., Scheller Bertram[5], M.D., Sauer Andreas[1,2], MS.c., Schaum Michael[6], M.Sc., Birkner Katharina[1,2], M.Sc., Singer Wolf[1,2,7], Ph.D., M.D., Wibral Michael[6], Ph.D., Uhlhaas Peter J.[1,2,8], Ph.D.

1. Department of Neurophysiology, Max Planck Institute for Brain Research, Frankfurt am Main, Germany.

2. Ernst Strüngmann Institute for Neuroscience (ESI) in cooperation with Max Planck Society (ESI), Frankfurt am Main, Germany.

3. School of Psychology, University of East London (UEL), London, UK.

4. Department of Neurology, Goethe University, Frankfurt am Main, Germany.

5. Clinic for Anesthesia, Intensive Care Medicine and Pain Therapy, Johann Wolfgang Goethe University Frankfurt am Main, Germany.

6. MEG Unit, Goethe University, Frankfurt am Main, Germany.

7. Frankfurt Institute for Advanced Studies (FIAS), Frankfurt am Main, Germany.

8. Institute of Neuroscience and Psychology, University of Glasgow, Glasgow, UK.

**Running Head title**: Ketamine-induced modulations of high frequency activity

**Keywords:** NMDA-receptor, ketamine, GABA, schizophrenia, MEG, gamma-band oscillations

**Number of words of the Abstract: 223**

**Number of words of the manuscript: 3009**

**Number of Tables: 0**

**Number of Figures: 5**

**Supplementary information: Yes**

**Correspondence:**

Dr. Peter J. Uhlhaas,

Institute of Neuroscience and Psychology

University of Glasgow

Hillead Str. 58

Glasgow, G12 8QB

E-Mail: peter.uhlhaas@glasgow.ac.uk

Tel: 0044/141 330 8730, Fax: 0044/141 330 8730

**Abstract**

Hypofunctioning of the N-methyl-D-aspartate (NMDA)-receptor (NMDA-R) has been prominently implicated in the pathophysiology of schizophrenia (ScZ). The current study tested the effects of ketamine, a dissociative anesthetic and NMDA-R antagonist, on resting-state activity recorded with magnetoencephalography (MEG) in healthy volunteers. In a single-blind cross-over design, each participant (n = 12) received, on two different sessions, a subanesthetic dose of S-ketamine (0.006 mg/Kg) and saline injection. MEG-data were analyzed at sensor- and source- level in the beta (13-30 Hz) and gamma (30-90 Hz) frequency ranges. In addition, connectivity analysis at source-level was performed using transfer entropy (TE). Ketamine increased gamma-power while beta-band activity was decreased. Specifically, elevated 30-90 Hz activity was pronounced in subcortical (thalamus and hippocampus) and cortical (frontal and temporal cortex) regions, whilst reductions in beta-band power were localized to the precuneus, cerebellum, anterior cingulate, temporal and visual cortex. TE analysis demonstrated increased information transfer in a thalamo-cortical network after ketamine administration. The findings are consistent with the pronounced dysregulation of high-frequency oscillations following the inhibition of NMDA-R in animal models of ScZ as well as with evidence from EEG-data in ScZ-patients and increased functional connectivity during early illness stages. Moreover, our data highlight the potential contribution of thalamo-cortical connectivity patterns towards ketamine-induced neuronal dysregulation, which may be relevant for the understanding of schizophrenia as a disorder of disinhibition of neural circuits.

**Keywords:** Ketamine, Neural Oscillations, MEG, Schizophrenia, Thalamus, Gamma-Band

**Clinical Trial registration:**

Trial name: EudraCT

Trial registry URL: https://eudract.ema.europa.eu/

Field Code Changed

Trial registration number: EudraCT number 2011-002937-21

## 1) Introduction

Schizophrenia (ScZ) is a debilitating psychiatric condition characterized by positive (e.g., hallucinations and delusions) and negative symptoms (e.g., flat affect), as well as cognitive deficits. Recent evidence suggests that a deficit in excitation/inhibition (E/I) balance parameters may constitute a pathophysiological mechanism that could underlie impairments in cognition and certain clinical symptoms (1). This is because during normal brain functioning, the generation of coherently organized large-scale networks is critically dependent upon the activity of gamma-aminobutyric acid (GABA) inhibitory interneurons expressing the calcium ($Ca^{2+}$) binding protein parvalbumin (PV) (2) and glutamatergic activation of PV interneurons (3), leading to rhythmic fluctuations of neuronal excitability at low and high-frequency ranges (4).

Specifically, NMDA-receptors number and functionality have been critically implicated in the pathophysiology of ScZ (5, 6) and abnormalities in glutamatergic transmission are a candidate mechanism for disturbed high frequency oscillations in the disorder. I*n-vivo* and *in-vitro* electrophysiological studies using NMDA-R antagonists have revealed an increase of spontaneous power at both low (30-60 Hz) and high (60-130 Hz) gamma-band ranges as well as at ripple frequencies (130-200 Hz) (7). In contrast, oscillations at lower-frequencies, such as in the theta-band, are reduced (7). Only a small number of studies have reported no effects (8) or a decrease (9). Different gamma-band frequencies, however, are not always equally modulated by ketamine and regional differences have been reported in some studies (8).

In the current study, we investigated the impact of ketamine on resting-state activity in MEG-recordings in healthy volunteers to establish links between pre-clinical research and findings from EEG/MEG-recordings in ScZ-patients. Recent evidence from spontaneous EEG recordings in ScZ-patients has reported increased spontaneous high-frequency activity in ScZ

(10, 11) although this has not been confirmed in all studies (10). In addition, several studies with functional magnetic resonance imaging (fMRI) indicated increased connectivity in large-scale networks following ketamine administration (12) which parallels findings in participants at-risk for psychosis and patients with first-episode ScZ (13).

Together with findings of elevated glutamate levels in early-stage ScZ (14), these findings raise the possibility that NMDA-hypofunctioning may underlie certain neuronal signatures of the disorder, highlighting the need to investigate the effects of Ketamine on gamma-band oscillations in healthy volunteers. However, in humans, only preliminary evidence exists on increased gamma-band power at rest following ketamine-administration at subanesthetic dosages (15).

## 2) Methods and Materials

### 2.1) *Participants*

Twelve participants (two females) with a mean age of 29.6 years (range: 27-39) were recruited and the structured Clinical Interview for DSM-IV (SCID-II) (16) was administered. If criteria were met for a past or present Axis I or II diagnosis or endorsed a family history of psychosis, the participant was excluded from the study. The medical screening consisted of a physical examination along with regular ECG, vital signs, blood tests, drug screening and psychological testing (see Supplementary Methods for a list of the tests adopted). The study was carried out according to the Declaration of Helsinki and approved by the ethical committees of the Goethe University Frankfurt. After complete description of the study to the participants, written informed consent was obtained.

2.4) *Experimental procedure*

**This study follows a single-blind, randomized, placebo-controlled, crossover design**. At the beginning of the experimental session, a bolus of 10 mg S-ketamine (drug condition) or 10 ml of NaCl 0.9% (placebo condition) was injected. This was followed by continuous intravenous infusion at 0.006 mg S-ketamine per Kg body weight per minute or NaCl 0.9%, respectively. We recorded eight minutes (four minutes with eyes open and four minutes with eyes closed) of resting-state activity during the continuous drug (ketamine or placebo) infusion. Only the eyes closed condition will be reported. Resting state activity was recorded circa 45 minutes after bolus injection, time in which participants performed a visual task (data not reported here). Following the MEG-recording, participants were examined using the Positive and Negative Syndrome Scale (PANSS) (17) with the addition of the 'disorganization' factor (18). **For each subject the placebo and ketamine conditions were completed between two and four weeks apart.**

2.5) *Anatomical MRI data acquisition*

Prior to the MEG-measurement, a high-resolution anatomical MRI scan was acquired for each participant using a 3D magnetization-prepared rapid-acquisition gradient echo sequence (160 slices; voxel size: 1x1x1 mm; FOV: 256 mm; TR: 2300 ms; TE: 3.93 ms). Scanning was performed using a 3-Tesla Siemens Trio scanner.

2.6) *MEG-data acquisition*

MEG data were acquired using a 275-sensors whole-head system (Omega 2005, VSM MedTech Ltd, BC, Canada) at a sampling rate of 600 Hz in a synthetic third order axial

gradiometer configuration. Data were band-passed filtered offline between 1-150 Hz, and participants' head movements were monitored before and after each recording using coils placed on the nasion and 1 cm anterior of the tragus of the left and right ear. Head movements were monitored before and after the recording. Recordings with movements larger than 5 mm were excluded from the analysis.

2.7) *MEG data processing and analysis*

Preprocessing and analysis of the MEG data was performed with the open source Matlab toolbox "FieldTrip" (19). The continuous recording was divided in segments of 2 seconds, each constituting a trial. Trials containing eye blinks or artifacts due to muscle activity or sensors (SQUIDs) jumps were discarded using automatic artifact rejection routines. Data were processed and statistically analyzed both at the sensor- and at the source-level. In addition, to investigate the effects of ketamine on the interactions between "drug-reactive" sources, we quantified changes in information transfer by measuring transfer entropy (TE) (20), as implemented in the TRENTOOL toolbox (21, 22).

2.7.1) *Sensor- and source- level analysis*

Sensor-level beta (13-30 Hz) and gamma (30-90 Hz) frequency activity was estimated using Morlet-wavelet convolution (5 cycles per wavelet). A non-parametric dependent samples *t*-test based on a permutation approach (1500 permutations) (23) was used to test differences between the placebo and ketamine conditions on all MEG sensors. To minimize the influence of differences in the distance between MEG-sensors and head position on amplitude

fluctuations, data was normalized both for high and low frequency analysis by dividing the amplitude of each frequency by the sum of the amplitudes of all frequencies.

Power-spectra were source-localized using a Dynamical Imaging of Coherent Sources (DICS) frequency beamformer (24). Single-subject source power estimates were normalized to the template brain of the Montreal Neurological Institute (MNI) using SPM8 (http://www.fil.ion.ucl.ac.uk/spm). Source data were statistically analyzed using cluster-based permutations (1500 permutations).

2.7.2) *Transfer Entropy (TE)*

Source-level functional connectivity between regions showing spectral changes after ketamine administration (see Results section below) was estimated using TE (25, 26). TE estimates the amount of information communicated from a source to a target process. This is achieved by quantifying how much information in the future of the target process is only predictable when knowing the past states of the source process. In this sense, TE can be seen as a more general, information theoretic version of Wiener-Granger causality (see Supplementary information for details on TE analysis). In the first step of our analysis, we extracted the time-course (i.e., virtual channels) of all sources showing ketamine-reactivity in the beta and gamma bands. We then assessed the global, drug-driven, change in TE between all sources through averaging TE values across all links per participant and conditions. To localize these changes across the links post-hoc, a one-sided permutation test for each link was performed and the alpha level was corrected for multiple comparisons using Bonferroni correction. Given the number of sources (n = 16) and the number of potential interactions for each source (n = 15), $p$ was set to 0.05 / 240 ($2.08 * 10^{-4}$). **In addition, we investigated TE-changes separately for interactions between sources in the beta- and gamma-frequency ranges as well as**

**between sources that were active in two different spectral bands (for this additional analysis, if no connectivity survived the Bonferroni-corrected threshold of $2.08 * 10^{-4}$, we adopted a more liberal threshold of $p < 0.0005$ uncorrected).**

3) **Results**

3.1) PANSS-Data

Ketamine lead to a statistically significant increase in all of the six PANSS subscales (see Figure 1 and Table S1).

3.2) *Sensors- and source- level MEG results*

After artifact rejection, 77 trials (SD = 21) remained in the placebo and 84 trials (SD = 12) in the ketamine condition. Ketamine administration caused an increase in gamma-band (30-90 Hz) power over frontal, parietal and temporal MEG sensors (see Figure 2). Similar to the sensor-level results, source-analysis demonstrated an increase in the gamma-band frequency range following ketamine administration in a number of cortical and subcortical regions. 30-90 Hz power was most prominently increased in the right hippocampus and right/left thalami, followed by cortical structures, such as the left fusiform gyrus, right medio frontal cortex, left frontal pole, left superior frontal gyrus, left superior temporal gyrus and left middle temporal gyrus (see Figure 3 and Table S2).

In contrast to gamma-band power, beta-band (13-30 Hz) activity was reduced after ketamine administration in particular over central MEG sensors. At the source-level, beta-band decreases were localized to the cerebellum, left/right precunei, right middle temporal

gyrus, left anterior cingulate cortex, right inferior temporal gyrus and visual cortex (see Figure 3 and Table S3).

3.3) *Correlation between MEG-source activity and PANNS*

Source-power in two anatomical regions showing the strongest ketamine effect in the gamma-band range (right hippocampus and right thalamus) were correlated to the PANSS subscales using a non-parametrical Spearman correlation. Results showed a negative correlation between right hippocampus power after ketamine injection and PANSS Positive scale ($rs(12) = -0.70$, $p = .011$).

3.4) *Transfer entropy results*

Ketamine administration caused an *increase* in the average TE-values (see Figure 5A for uncorrected effects). Connections that survived multiple comparisons correction were localized to links from left middle temporal gyrus (MTG-L) to right inferior temporal gyrus (ITG-R); ITG-R to the left Thalamus (Th-L, ); Th-L to right visual cortex (Visual Cortex-R); Visual Cortex-R to right precuneus (Prec-R); Prec-R to Th-L (Figure 5B). Connections with significant increases in information transfer were found for source pairs comprising three of four possible types: between sources with ketamine-induced changes in the beta-band, between sources with changes in the gamma band, and from sources with changes in the gamma band to sources with changes in the beta band. Changes in TE values for the remaining type, from sources with changes in the beta band to sources with changes in the gamma band were found at slightly less conservative thresholds of $p < 0.0005$ (Figure 5D).

For the purpose of comparison we also present the other connection types at this threshold (Figure 5C-E).

4) **Discussion**

There is increasing evidence suggesting that core features of ScZ may be the consequence of hypofunctioning of NMDA-receptors (5). In the current study, we investigated the effects of ketamine, a noncompetitive antagonist of the NMDA-R, on resting-state MEG-activity in healthy volunteers, to establish whether changes in amplitude fluctuations and connectivity patterns following ketamine administration allow links to the pathophysiology of ScZ. Currently, only preliminary evidence exists on the effects of ketamine in humans on spontaneous beta/gamma-band activity (15). Our findings of pronounced increases in gamma-band power and increased functional connectivity are in agreement with extensive pre-clinical data on the effects of ketamine on neural oscillations (27-32). Moreover, there are similarities with evidence from EEG and fMRI-recordings in ScZ (13, 33), which together have potentially important implications for the understanding of ScZ as a disorder involving fundamentally a disinhibition of cortico-subcortical circuits.

**Ketamine Effects on High-frequency activity: Potential neurophysiological mechanisms**

The spectra during resting-state activity corresponded to the usual 1/f distribution both in the placebo and in the ketamine condition. The contrast between ketamine-induced spectral activity and the placebo condition, however, suggests an upregulation of high-frequency activity with a peak ~ 60 Hz (Figure 4). The frequency as well as the magnitude of this effect are comparable to visually-induced activity that has been described in recent MEG-studies

(34), suggesting that NMDA-R hypofunctioning could be associated with an oscillatory process in cortical and subcortical regions. In contrast to 30-90 Hz power, beta-band activity was strongly reduced, which is in agreement with recent data (35).

Source-reconstruction of resting-state MEG-activity allowed us to determine the neural generators in different frequency ranges. In the 30-90 Hz frequency band, ketamine caused an upregulation in subcortical and cortical areas. The largest increases of gamma-band activity were observed in the right hippocampus and right/left thalami, followed by parietal, temporal and frontal structures (Figure 3). This is in agreement with previous *in-vivo* studies in rodents (9, 27, 36-38), which consistently demonstrated a ketamine-induced increase in spontaneous gamma-band activity in cortical and subcortical areas. Decreases in beta-band were localized to brain regions that were overall distinct from gamma-band generators. Maximal reductions in 13-30 Hz were localized, for example, to the cerebellum, temporal and visual cortex.

Potential mechanisms for the ketamine-driven upregulation of gamma-band activity are increased excitability of pyramidal cells due to reduced activation of GABAergic interneurons and a shift in the relative contribution of AMPA and NMDA-R mediated excitatory post synaptic potentials (EPSPs) to the drive of interneurons (39). Previous studies have shown that NMDA-R hypofunction leads to an increase in firing rate of pyramidal neurons (40). In addition, AMPA receptor mediated excitation becomes relatively more preponderant when NMDA-Rs are deficient as AMPA-R mediated EPSPs have much faster kinetics than NMDA-R mediated EPSPs and are more numerous than NMDA-Rs on $PV^{+}$-interneurons (41). Accordingly, reducing the NMDA-R mediated excitatory input on GABAergic interneurons increases the ratio of fast over slow EPSPs (39) and this, together with increased activity of pyramidal cells, provides favorable conditions for fast oscillations with important implications for information processing and network-interactions.

Gamma-band oscillations are particularly prominent in superficial layers (layers 2/3) (42), the main origin of feedforward projections, and are dependent upon fast, transient excitation of fast-spiking interneurons (43). In contrast, beta oscillations are largely found in infragranular layers and can be independent of excitatory or inhibitory synaptic transmission (44). Current theories suggest that beta-band oscillations are therefore involved in the mediation of feedback to lower sensory areas and important for predictive coding processes (45). Accordingly, one effect of the NMDA-R hypofunctioning is a possible shift towards feed-forward mediated information transmission and/or increase in background activity which could interfere with incoming sensory information. As a result, a decrease in signal-to-noise in neural circuits occurs (46, 47), which could impact upon the ability to differentiate between relevant and irrelevant information, a symptom commonly observed in the early stages of ScZ (48).

This hypothesis is supported by our result of increase functional connectivity (TE) between sources, which included the thalamus, hippocampus, parietal and temporal cortices. Increased TE-values have to be interpreted as information in one source closely following information available in another source (26). Thus, at an information theoretical level, our data suggests that MEG-derived generators follow more readily the input they receive, which could further amplify the shift towards a higher-frequency regime and thus contribute to a breakdown of filtering capabilities with respect to a source's input.

**Interestingly, elevated hippocampal gamma-band activity after ketamine administration correlated negatively with positive symptoms as measured with PANSS, which contrasts with findings in ScZ-patients indicating an opposite relationship (49). One possibility is that elevated hippocampal gamma-band activity during acute ketamine administration indexes an initial mechanism to compensate for dysfunctional**

**thalamo-cortical sensory transmission through enhanced gating of neuronal responses, a process that is least in part mediated by hippocampal interneurons (50), and thus reduce the occurrence of psychotic symptoms.**

**NMDA-R, Gamma-Band Activity, Network Organization and ScZ**

An important question concerns the similarities between the changes in rhythmic activity and connectivity patterns resulting from NMDA-R hypofunction in the current study and the evidence on abnormal large-scale network-activity in ScZ-patients. As pointed above, ketamine and associated NMDA-R hypofunction lead to an upregulation of high-frequency activity and increased interactions between nodes of the network.

Currently, the large majority of studies in patients with ScZ have reported decreases of task related gamma band power (51) and connectivity (52, 53). However, a recent study (33) showed that background gamma activity is increased during auditory steady-state stimulation in SZ which was interpreted as a disruption in E/I-balance parameters. This is furthermore supported by preliminary evidence for increased gamma-band in medication-naïve first-episode ScZ-patients at-rest (11, 54) which has not, however, been confirmed in other studies (10, 51, 55).

Additional evidence supporting the relationship between the role of glutamatergic abnormalities and neurophysiological dysfunctions in ScZ comes from several studies that have examined functional connectivity in early-stage ScZ with resting-state fMRI. Consistent with our finding of increased connectivity in thalamo-cortical circuits, individuals at high risk for ScZ and patients with early-course ScZ were characterized by increased connectivity which was not present in chronic ScZ-patients (13).

The possibility of NMDA-R mediated disinhibition in ScZ at illness-onset is supported by our recent data in unmedicated first-episode-ScZ patients which suggests an excessive spreading of neural activity as indexed by event-related fields during sensory processing in MEG-data (56), as well as by findings suggesting elevated glutamate levels during early illness stages which decrease progressively with illness duration (14). Accordingly, these findings highlight the possibility of a stage-specific elevation of network-activity and organization, which is compatible with a large-scale disinhibition of neural circuits in ScZ.

Our results of MEG-informed source-localization furthermore are consistent with recent data that have highlighted the importance of thalamo-cortical interactions and hippocampal circuits in the pathophysiology of ScZ. Several resting-state fMRI studies reported increased functional connectivity between thalamus and cortical regions (57-59), albeit some report mixed findings (59). In addition, the increase in gamma-band activity in hippocampal sources, a brain region with a large number of NMDA-receptor sites (60), is consistent with findings highlighting the possible contribution of elevated metabolism as a result of NMDA-R hypofunctioning in the early stages of ScZ (61).

**Issues for further Research and Limitations**

It should be noted that the interpretation of the physiological effects of ketamine is complicated by the fact that, in addition to blocking NMDA-Rs, ketamine also increases the systemic levels of dopamine, acetylcholine, and norepinephrine (62). However, more recent evidence suggests that the increase in gamma-band activity is mainly due to a specific blockade of NMDA receptors containing the NR2A subunit (63).

In addition, several brain regions with significant modulation at beta/gamma-band frequencies were localized to subcortical areas (thalamus and hippocampus). Albeit MEG subcortical source localization remains challenging due to the rapid decay of the neuromagnetic field, recent studies have however reported robust signals obtained from thalamic and hippocampal sources (64-66), suggesting the potential suitability of MEG to detect rhythmic activity from deeper brain regions.

The important role of the thalamus in the dysregulation of high-frequency oscillations in our MEG-data is supported by previous findings showing that the thalamus is centrally involved in the regulation of synchronous cortical activity and in the gating of sensory information (67). Specifically, there is a large body of evidence showing that gamma-band oscillations are robust signature of thalamic activity as indicated by pacemaker function of cells in the thalamic reticular nucleus (RT) (68), and pronounced 30-90 Hz oscillations in the lateral geniculate nucleus (LGN) (69). Moreover, data from animal model indicate that ketamine reduces extracellular GABA levels by acting on NMDA-R PV interneurons (70). In particular, GABA release reduction from the RT to other thalamic nuclei, due to inactivation of NMDA-R on RT-neurons, would lead to increase firing rate of thalamic relay neurons and pathological activation of thalamo-cortical circuits, which could trigger a widespread shift in excitability levels (71).

This evidence is consistent with current findings of thalamic-driven dysregulation of connectivity patterns following acute ketamine administration (72). Together, these findings highlight an important convergence between pre-clinical findings and MEG-reconstructed resting-state networks that identify the thalamus as a core region of ketamine-induced network changes. Moreover, NMDA-R blockade by ketamine increases global-based

connectivity (12) and increased functional inputs to regions such as the thalamus, frontal lobe and occipital cortex, in human fMRI resting-state recordings.

**Summary**

The findings of the current study support previous data from invasive electrophysiological investigations, which have demonstrated a profound effect of NMDA-hypofunction on coordinated high-frequency activity (7, 29). Because some evidence suggests that spontaneous gamma-band power may be increased in ScZ-patients, especially at illness-onset (73), and because gamma-band activity is constitutive for cognition and normal brain functions (1), it is important to further identify the mechanisms through which ketamine leads to the upregulation of gamma-band activity. This will require an integration of both targeted pharmacological studies in *in-vitro* and *in-vivo* preparations as well as further investigations of the connectivity and dynamics of large-scale neuronal networks. Further research into the mechanisms underlying the effects of NMDA-R on high-frequency activity promises insights into the role of beta/gamma-band oscillations for normal brain functions, the pathophysiology of ScZ, but also of affective disorders, such as depression, since ketamine has recently been demonstrated to act rapidly as an anti-depressant (74).

**Acknowledgments**

We wish to thank Alla Brodski and Patricia Wollstadt for their support in the data processing and analysis. In addition, we would like to acknowledge the helpful suggestions of Prof. Boris Quednow in regards to the design of the study.

**Funding**

D.R. was supported by the LOWE grant *Neuronale Koordination Forschungsschwerpunkt Frankfurt* (NeFF).

**Conflict of Interest statement**

PJU has received research support from Lilly.

**References**

1. Uhlhaas PJ, Singer W (2012): Neuronal dynamics and neuropsychiatric disorders: Towards a translational paradigm for dysfunctional large-scale networks. *Neuron*. 75:963-980.

2. Sohal VS, Zhang F, Yizhar O, Deisseroth K (2009): Parvalbumin neurons and gamma rhythms enhance cortical circuit performance. *Nature*. 459:698-702.

3. Whittington MA, Traub RD, Jefferys JG (1995): Synchronized oscillations in interneuron networks driven by metabotropic glutamate receptor activation. *Nature*. 373:612-615.

4. Wang XJ (2010): Neurophysiological and computational principles of cortical rhythms in cognition. *Physiological reviews*. 90:1195-1268.

5. Moghaddam B, Javitt D (2012): From revolution to evolution: the glutamate hypothesis of schizophrenia and its implication for treatment. *Neuropsychopharmacology : official publication of the American College of Neuropsychopharmacology*. 37:4-15.

6. Kirov G, Pocklington AJ, Holmans P, Ivanov D, Ikeda M, Ruderfer D, et al. (2012): De novo CNV analysis implicates specific abnormalities of postsynaptic signalling complexes in the pathogenesis of schizophrenia. *Mol Psychiatry*. 17:142-153.

7. Hunt MJ, Kasicki S (2013): A systematic review of the effects of NMDA receptor antagonists on oscillatory activity recorded in vivo. *J Psychopharmacol*.

8. Wood J, Kim Y, Moghaddam B (2012): Disruption of prefrontal cortex large scale neuronal activity by different classes of psychotomimetic drugs. *The Journal of neuroscience : the official journal of the Society for Neuroscience*. 32:3022-3031.

9. Hunt MJ, Falinska M, Leski S, Wojcik DK, Kasicki S (2011): Differential effects produced by ketamine on oscillatory activity recorded in the rat hippocampus, dorsal striatum and nucleus accumbens. *J Psychopharmacol*. 25:808-821.

10. Rutter L, Carver FW, Holroyd T, Nadar SR, Mitchell-Francis J, Apud J, et al. (2009): Magnetoencephalographic gamma power reduction in patients with schizophrenia during resting condition. *Human brain mapping*. 30:3254-3264.

11. Kikuchi M, Hashimoto T, Nagasawa T, Hirosawa T, Minabe Y, Yoshimura M, et al. (2011): Frontal areas contribute to reduced global coordination of resting-state gamma activities in drug-naive patients with schizophrenia. *Schizophr Res*. 130:187-194.

12. Driesen NR, McCarthy G, Bhagwagar Z, Bloch M, Calhoun V, D'Souza DC, et al. (2013): Relationship of resting brain hyperconnectivity and schizophrenia-like symptoms produced by the NMDA receptor antagonist ketamine in humans. *Mol Psychiatry*.

13. Anticevic A, Corlett PR, Cole MW, Savic A, Gancsos M, Tang Y, et al. (in press): NMDA Receptor Antagonist Effects on Prefrontal Cortical Connectivity Better Model Early Than Chronic Schizophrenia. *Biological Psychiatry*.

14. Marsman A, van den Heuvel MP, Klomp DW, Kahn RS, Luijten PR, Hulshoff Pol HE (2013): Glutamate in schizophrenia: a focused review and meta-analysis of (1)H-MRS studies. *Schizophrenia bulletin*. 39:120-129.

15. Schwartz MS, Virden S, Scott DF (1974): Effects of ketamine on electroencephalograph. *Anaesthesia*. 29:135-140.

16. First MB, Gibbon M, Spitzer RL, Williams JBW, Benjamin LS (1997): Structured Clinical Interview for DSM-IV Axis II Personality Disorders, (SCID-II). *Washington, DC: American Psychiatric Press, Inc, 1997*.

17. Kay SR, Fiszbein A, Opler LA (1987): The positive and negative syndrome scale (PANSS) for schizophrenia. *Schizophrenia bulletin*. 13:261-276.

18. Cuesta MJ, Peralta V (1995): Cognitive disorders in the positive, negative, and disorganization syndromes of schizophrenia. *Psychiatry research*. 58:227-235.

19. Oostenveld R, Fries P, Maris E, Schoffelen J-M (2011): FieldTrip: Open source software for advanced analysis of MEG, EEG, and invasive electrophysiological data. *Computational intelligence and neuroscience*. vol. 2011, Article ID 156869:9 pages, 2011. doi:2010.1155/2011/156869

20. Schreiber T (2000): Measuring information transfer. *Physics reviews Letters*. 85:461-464.

21. Lindner M, Vicente R, Priesemann V, Wibral M (2011): TRENTOOL: A Matlab open source toolbox to analyse information flow in time series data with transfer entropy. *BMC neuroscience*. 18:12:119.

22. Wollstadt P, Martinez-Zarzuela M, Vicente R, Diaz-Pernas F, Wibral M (in press): Efficient transfer entropy analysis of non-stationary neural time series. *PLoS ONE*.

23. Maris E, Oostenveld R (2007): Nonparametric statistical testing of EEG- and MEG-data. *Journal of Neuroscience Methods*. 164:177-190.

24. Gross J (2001): Dynamic imaging of coherent sources: Studying neural interactions in the human brain. *Proceedings of the National Academy of Sciences*. 98:694-699.

25. Wibral M, Vicente R, Lindner M (2014): Transfer Entropy in Neuroscience. In: Springer, editor. *Directed Information Measures in Neuroscience*. Berlin Heidelberg: Springer.

26. Wibral M, Pampu N, Priesemann V, Siebenhühner F, Seiwert H, Linder M, et al. (2013): Measuring information-transfer delays. *PLoS One*. 8:e55809.

27. Pinault D (2008): N-methyl d-aspartate antagonists ketamine and MK-801 induce wake-related aberrant gamma oscillations in the rat neocortex. *Biological Psychiatry*. 63:730-735.

28. Kittelberger K, Hur EE, Sazegar S, Keshavan V, Kocsis B (2012): Comparison of the effects of acute and chronic administration of ketamine on hippocampal oscillations:

relevance for the NMDA receptor hypofunction model of schizophrenia. *Brain structure & function*. 217:395-409.

29. Kocsis B, Brown RE, McCarley RW, Hajos M (2013): Impact of ketamine on neuronal network dynamics: translational modeling of schizophrenia-relevant deficits. *CNS Neurosci Ther*. 19:437-447.

30. Zhang Y, Yoshida T, Katz DB, Lisman JE (2012): NMDAR antagonist action in thalamus imposes delta oscillations on the hippocampus. *Journal of neurophysiology*. 107:3181-3189.

31. Hakami T, Jones NC, Tolmacheva EA, Gaudias J, Chaumont J, Salzberg M, et al. (2009): NMDA receptor hypofunction leads to generalized and persistent aberrant gamma oscillations independent of hyperlocomotion and the state of consciousness. *PLoS One*. 4:e6755.

32. Caixeta FV, Cornelio AM, Scheffer-Teixeira R, Ribeiro S, Tort AB (2013): Ketamine alters oscillatory coupling in the hippocampus. *Scientific reports*. 3:2348.

33. Hirano Y, Oribe N, Kanba S, Onitsuka T, Nestor PG, Spencer KM (2015): Spontaneous Gamma Activity in Schizophrenia. *JAMA psychiatry*.

34. Hoogenboom N, Schoffelen JM, Oostenveld R, Parkes LM, Fries P (2006): Localizing human visual gamma-band activity in frequency, time and space. *NeuroImage*. 29:764-773.

35. Lazarewicz MT, Ehrlichman RS, Maxwell CR, Gandal MJ, Finkel LH, Siegel SJ (2010): Ketamine modulates theta and gamma oscillations. *Journal of cognitive neuroscience*. 22:1452-1464.

36. Zhang Y, Yoshida T, Katz DB, Lisman JE (2012): NMDAR antagonist action in the thalamus imposes oscillations on the hippocampus. *Journal of Neurophysiology*. 107:3181-3189.

37. Ehrlichman RS, Gandal MJ, Maxwell CR, Lazarewicz MT, Finkel LH, Contreras D, et al. (2009): N-methyl-d-aspartic acid receptor antagonist-induced frequency oscillations in mice recreate pattern of electrophysiological deficits in schizophrenia. *Neuroscience*. 158:705-712.

38. Phillips KG, Cotel MC, McCarthy AP, Edgar DM, Tricklebank M, O'Neill MJ, et al. (2012): Differential effects of NMDA antagonists on high frequency and gamma EEG oscillations in a neurodevelopmental model of schizophrenia. *Neuropharmacology*. 62:1359-1370.

39. Rotaru DC, Yoshino H, Lewis DA, Ermentrout GB, Gonzalez-Burgos G (2011): Glutamate receptor subtypes mediating synaptic activation of prefrontal cortex neurons: relevance for schizophrenia. *The Journal of neuroscience : the official journal of the Society for Neuroscience*. 31:142-156.

40. Homayoun H, Moghaddam B (2007): NMDA receptor hypofunction produces opposite effects on prefrontal cortex interneurons and pyramidal neurons. *The Journal of neuroscience : the official journal of the Society for Neuroscience*. 27:11496-11500.

41. Gonzalez-Burgos G, Lewis DA (2012): NMDA receptor hypofunction, parvalbumin-positive neurons, and cortical gamma oscillations in schizophrenia. *Schizophrenia bulletin*. 38:950-957.

42. Buffalo EA, Fries P, Landman R, Buschman TJ, Desimone R (2011): Laminar differences in gamma and alpha coherence in the ventral stream. *Proceedings of the National Academy of Sciences of the United States of America*. 108:11262-11267.

43. Whittington MA, Traub RD (2003): Interneuron diversity series: inhibitory interneurons and network oscillations in vitro. *Trends Neurosci*. 26:676-682.

44. Roopun AK, Cunningham MO, Racca C, Alter K, Traub RD, Whittington MA (2008): Region-specific changes in gamma and beta2 rhythms in NMDA receptor dysfunction models of schizophrenia. *Schizophrenia bulletin*. 34:962-973.

45. Arnal LH, Giraud AL (2012): Cortical oscillations and sensory predictions. *Trends in cognitive sciences*. 16:390-398.

46. Kulikova SP, Tolmacheva EA, Anderson P, Gaudias J, Adams BE, Zheng T, et al. (2012): Opposite effects of ketamine and deep brain stimulation on rat thalamocortical information processing. *The European journal of neuroscience*. 36:3407-3419.

47. Saunders JA, Gandal MJ, Siegel SJ (2012): NMDA antagonists recreate signal-to-noise ratio and timing perturbations present in schizophrenia. *Neurobiol Dis*. 46:93-100.

48. McGhie A, Chapman J (1961): Disorders of attention and perception in early schizophrenia. *The British journal of medical psychology*. 34:103-116.

49. Lahti AC, Weiler MA, Holcomb HH, Tamminga CA, Carpenter WT, McMahon R (2006): Correlations between rCBF and symptoms in two independent cohorts of drug-free patients with schizophrenia. *Neuropsychopharmacology : official publication of the American College of Neuropsychopharmacology*. 31:221-230.

50. Miller CL, Freedman R (1995): The activity of hippocampal interneurons and pyramidal cells during the response of the hippocampus to repeated auditory stimuli. *Neuroscience*. 69:371-381.

51. Gruetzner C, Wibral M, Sun L, Rivolta D, Maurer K, Singer W, et al. (2013): Deficits in high- (> 60 Hz) gamma band oscillations during visual processing in schizophrenia. *Frontiers in human neuroscience*. 7:DOI: 10.3389/fnhum.2013.00088.

52. Uhlhaas PJ, Linden DE, Singer W, Haenschel C, Lindner M, Maurer K, et al. (2006): Dysfunctional long-range coordination of neural activity during Gestalt perception in

schizophrenia. *The Journal of neuroscience : the official journal of the Society for Neuroscience*. 26:8168-8175.

53. Spencer KM, Nestor PG, Niznikiewicz MA, Salisbury DF, Shenton ME, McCarley RW (2003): Abnormal neural synchrony in schizophrenia. *The Journal of neuroscience : the official journal of the Society for Neuroscience*. 23:7407-7411.

54. Spencer KM, Niznikiewicz MA, Nestor PG, Shenton ME, McCarley RW (2009): Left auditory cortex gamma synchronization and auditory hallucination symptoms in schizophrenia. *BMC neuroscience*. 10:85.

55. Sun L, Castellanos N, Grutzner C, Koethe D, Rivolta D, Wibral M, et al. (2013): Evidence for dysregulated high-frequency oscillations during sensory processing in medication-naive, first episode schizophrenia. *Schizophr Res*. 150:519-525.

56. Rivolta D, Castellanos NP, Stawowsky C, Helbling S, Wibral M, Grutzner C, et al. (2014): Source-reconstruction of event-related fields reveals hyperfunction and hypofunction of cortical circuits in antipsychotic-naive, first-episode schizophrenia patients during Mooney face processing. *The Journal of neuroscience : the official journal of the Society for Neuroscience*. 34:5909-5917.

57. Klingner CM, Langbein K, Dietzek M, Smesny S, Witte OW, Sauer H, et al. (2014): Thalamocortical connectivity during resting state in schizophrenia. *European archives of psychiatry and clinical neuroscience*. 264:111-119.

58. Anticevic A, Cole MW, Repovs G, Murray JD, Brumbaugh MS, Winkler AM, et al. (2013): Characterizing Thalamo-Cortical Disturbances in Schizophrenia and Bipolar Illness. *Cerebral cortex (New York, NY : 1991)*.

59. Woodward ND, Karbasforoushan H, Heckers S (2012): Thalamocortical dysconnectivity in schizophrenia. *The American journal of psychiatry*. 169:1092-1099.

60. Monaghan DT, Cotman CW (1985): Distribution of N-methyl-D-aspartate-sensitive L-[3H]glutamate-binding sites in rat brain. *The Journal of neuroscience : the official journal of the Society for Neuroscience*. 5:2909-2919.

61. Schobel SA, Chaudhury NH, Khan UA, Paniagua B, Styner MA, Asllani I, et al. (2013): Imaging patients with psychosis and a mouse model establishes a spreading pattern of hippocampal dysfunction and implicates glutamate as a driver. *Neuron*. 78:81-93.

62. Gunduz-Bruce H (2009): The acute effects of NMDA antagonism: from the rodent to the human brain. *Brain Res Rev*. 60:279-286.

63. Kocsis B (2012): Differential role of NR2A and NR2B subunits in N-methyl-D-aspartate receptor antagonist-induced aberrant cortical gamma oscillations. *Biol Psychiatry*. 71:987-995.

64. Ribary U, Ioannides AA, Singh KD, Hasson R, Bolton JP, Lado F, et al. (1991): Magnetic field tomography of coherent thalamocortical 40-Hz oscillations in humans. *Proc Natl Acad Sci U S A*. 88:11037-11041.

65. Poch C, Fuentemilla L, Barnes GR, Duzel E (2011): Hippocampal theta-phase modulation of replay correlates with configural-relational short-term memory performance. *J Neurosci*. 31:7038-7042.

66. Roux F, Wibral M, Singer W, Aru J, Uhlhaas PJ (2013): The phase of thalamic alpha activity modulates cortical gamma-band activity: evidence from resting-state MEG recordings. *The Journal of neuroscience : the official journal of the Society for Neuroscience*. 33:17827-17835.

67. Saalmann YB, Kastner S (2011): Cognitive and perceptual functions of the visual thalamus. *Neuron*. 71:209-223.

68. Pinault D, Deschenes M (1992): Control of 40-Hz firing of reticular thalamic cells by neurotransmitters. *Neuroscience*. 51:259-268.

69. Ghose GM, Freeman RD (1992): Oscillatory discharge in the visual system: does it have a functional role? *Journal of neurophysiology*. 68:1558-1574.

70. Grasshoff C, Gillessen T, Wagner E, Thiermann H, Szinicz L (2005): Ketamine reduces cholinergic modulated GABA release from rat striatal slices. *Toxicology letters*. 156:361-367.

71. Ferrarelli F, Tononi G (2011): The thalamic reticular nucleus and schizophrenia. *Schizophrenia bulletin*. 37:306-315.

72. Dawson N, McDonald M, Higham DJ, Morris BJ, Pratt JA (2014): Subanesthetic ketamine treatment promotes abnormal interactions between neural subsystems and alters the properties of functional brain networks. *Neuropsychopharmacology : official publication of the American College of Neuropsychopharmacology*. 39:1786-1798.

73. Kim SY, Lee H, Kim HJ, Bang E, Lee SH, Lee DW, et al. (2011): In vivo and ex vivo evidence for ketamine-induced hyperglutamatergic activity in the cerebral cortex of the rat: Potential relevance to schizophrenia. *NMR Biomed*. 24:1235-1242.

74. Berman RM, Cappiello A, Anand A, Oren DA, Heninger GR, Charney DS, et al. (2000): Antidepressant effects of ketamine in depressed patients. *Biol Psychiatry*. 47:351-354.

**Figure legends**

**Figure 1.** Average scores on the six different PANSS subscales for the placebo (black) and ketamine (gray) conditions. Error bars indicate the s.e.m. (* = $p < .05$).

**Figure 2**. Sensor-level analysis. (A) Topoplots representing the average power spectra (fT) of gamma (top) and beta (bottom) frequency ranges in the placebo (left) and ketamine (right) conditions. (B) Results of the non-parametric cluster-based statistic highlighting sensors showing a statistically significant effect for gamma (top) and beta (bottom) frequencies (red: ketamine > placebo; blue: colors placebo > ketamine) (* = $p < .001$).

**Figure 3.** Source-level analysis. Cluster-based non-parametric statistic highlights statistically significant differences between the placebo and ketamine condition across the gamma (left) and beta (right) frequency bands (red: ketamine > placebo; blue: placebo > ketamine). *Gamma-band* (30-90 Hz): 1. R-hippocampus [10 -10 -20], 2. R-thalamus [10 -10 10], 3. L-thalamus [-10 -20 10], 4. L-fusiform gyrus [-40 -10 -30], 5. R-medial frontal cortex [0 40 -20], 6. L-frontal pole [-20 40 -10], 7. L-superior frontal gyrus [-20 40 40], 8. L-superior temporal gyrus [-70 -20 0], 9. L-middle temporal gyrus [-60 0 -30]. *Beta-band* (13-30 Hz): 1. cerebellum [0 -40 -20], 2. L-precuneus [-20 -50 20], 3. R-precuneus [30 -50 10], 4. R-middle temporal gyrus [60 -30 -10], 5. L-anterior cingulate [0 20 -10], 6. R-inferior temporal gyrus [50 -60 -20], 7. R-visual cortex [30 -90 -10].

**Figure 4**. Power spetra analysis. (Left) Placebo and ketamine power-spectra as averaged across all subjects and calculated considering all MEG sensors (shades indicated the s.e.m.). (Right) Relative change (i.e., ((Ketamine power – Placebo power) / Placebo power) * 100) of the ketamine power with respect to the placebo power in the gamma-band range.

**Figure 5.** Transfer entropy (TE) analysis. TE differences between ketamine and placebo conditions. Green diamonds indicate MEG sources reactive to ketamine in the gamma band, blue circles indicate sources reactive in the beta band (see Figure 3). Arrow colors indicate strength of the difference. (A) Uncorrected differences in TE. (B) Statistically significant differences (Bonferroni corrected: $p < 2.08*10^{-4}$). For illustration purposes we also provide the TE differences at a significance threshold of $p < 0.0005$ uncorrected, for the transfer entropy between (C) sources reactive in the beta frequency band, (D) in the gamma frequency band, and (E) between beta- and gamma-sources. Legend: FrontalPole-L = left frontal pole, MFC = medial frontal cortex, SFG-L = left superior frontal gyrus, ACC = anterior cingulate cortex, MTG-L = left middle temporal gyrus, FuG-L = left fusiform gyrus, Th-L= left thalamus, Cb = cerebellum, Prec-L = left precuneus, HI-R = right hippocampus, Th-R = right thalamus, MTG-R = right medial temporal gyrus,Prec-R = right precuneus, ITG-R = right inferior temporal gyrus, VisualCortex-R = right visual cortex.

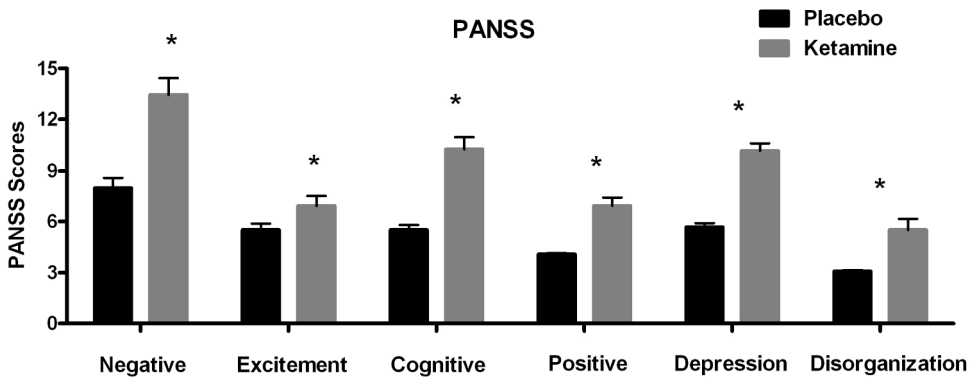


Figure 1. Average scores on the six different PANSS subscales for the placebo (black) and ketamine (gray) conditions. Error bars indicate the s.e.m. (* = $p < .05$).
197x80mm (300 x 300 DPI)

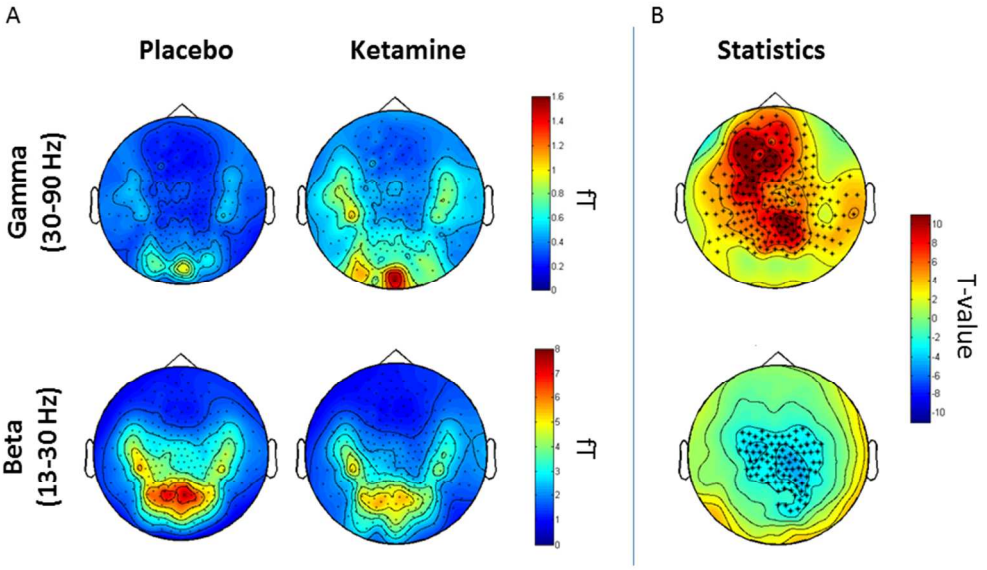


Sensor-level analysis. (A) Topoplots representing the average power spectra (fT) of gamma (top) and beta (bottom) frequency ranges in the placebo (left) and ketamine (right) conditions. (B) Results of the non-parametric cluster-based statistic highlighting sensors showing a statistically significant effect for gamma (top) and beta (bottom) frequencies. Red colors indicate a statistically significant difference in favor of the ketamine condition, whereas blue colors indicate a difference in favor of the placebo condition (* = p < .001).
245x147mm (96 x 96 DPI)

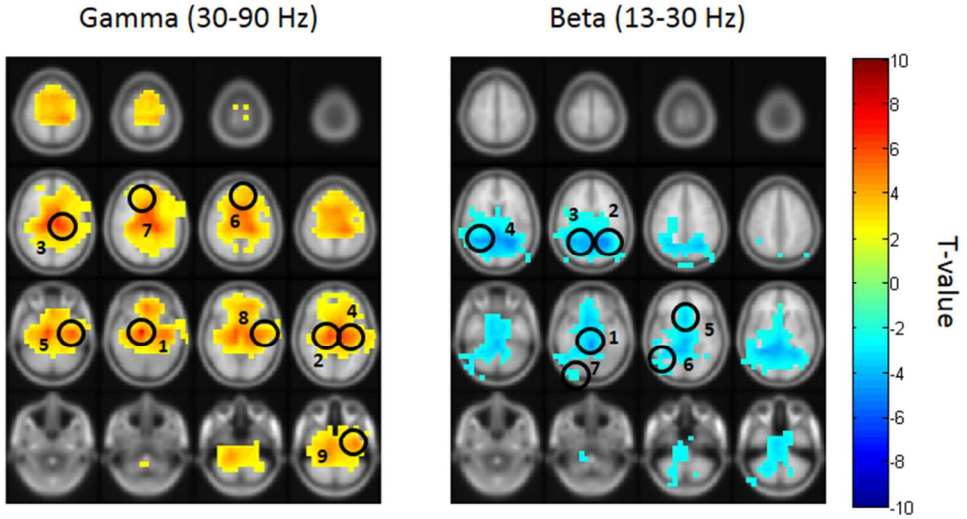


201x110mm (96 x 96 DPI)

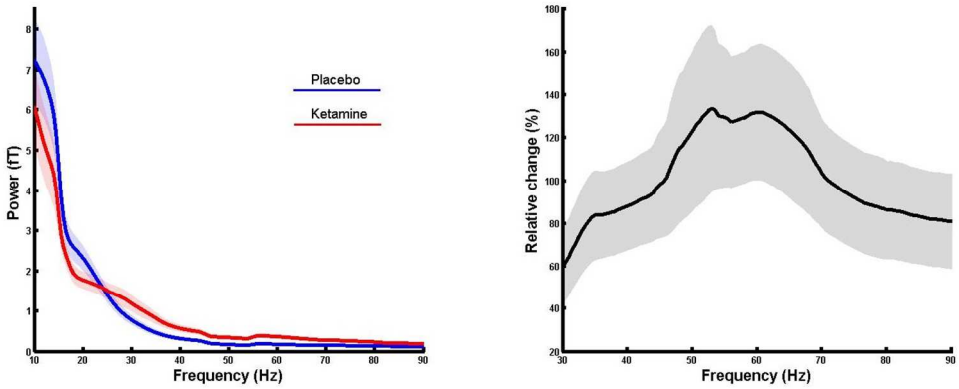


Power spetra analysis. (A) Placebo and ketamine power-spectra as averaged across all subjects and calculated considering all MEG sensors (shades indicated the s.e.m.). (B) Relative change (i.e., ((Ketamine power – Placebo power) / Placebo power) * 100) of the ketamine power with respect to the placebo power in the gamma-band range.
371x154mm (96 x 96 DPI)

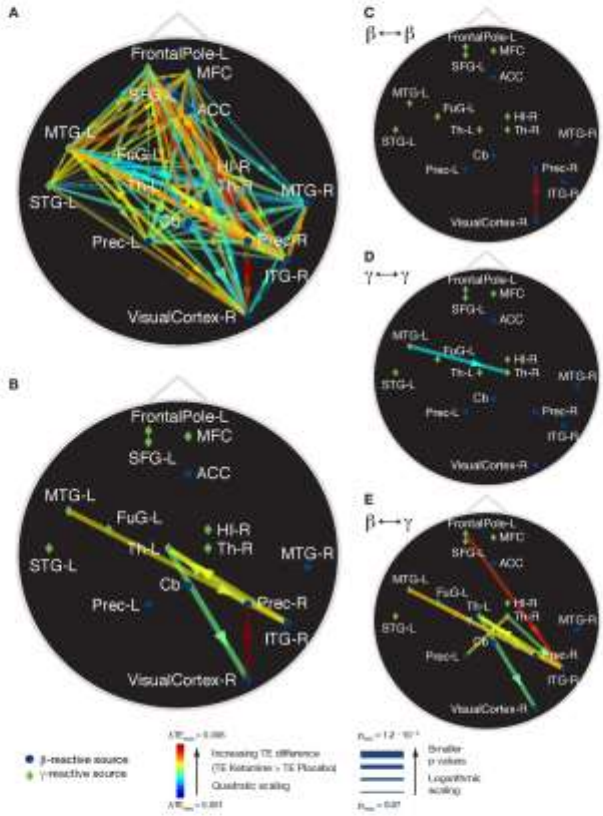


Transfer entropy (TE) analysis. TE differences between ketamine and placebo conditions. Green diamonds indicate MEG sources reactive to ketamine in the gamma band, blue circles indicate sources reactive in the beta band (see Figure 3). Arrow colors indicate strength of the difference. (A) Uncorrected differences in TE. (B) Statistically significant differences (Bonferroni corrected: $p < 2.08*10\text{-}4$). For illustration purposes we also provide the TE differences at a significance threshold of $p < 0.0005$ uncorrected, for the transfer entropy between (C) sources reactive in the beta frequency band, (D) in the gamma frequency band, and (E) between beta- and gamma-sources. Legend: FrontalPole-L = left frontal pole, MFC = medial frontal cortex, SFG-L = left superior frontal gyrus, ACC = anterior cingulate cortex, MTG-L = left middle temporal gyrus, FuG-L = left fusiform gyrus, Th-L= left thalamus, Cb = cerebellum, Prec-L = left precuneus, HI-R = right hippocampus, Th-R = right thalamus, MTG-R = right medial temporal gyrus,Prec-R = right precuneus, ITG-R = right inferior temporal gyrus, VisualCortex-R = right visual cortex.

209x297mm (300 x 300 DPI)

# Supplementary material

## Supplementary Tables

**Table S1.** PANSS scores for the placebo and the ketamine condition. Indicated are average, standard error of the mean (SEM) and *t*-test statistics.

| | Placebo | | Ketamine | | |
|---|---|---|---|---|---|
| | Average | SEM | Average | SEM | *t*-test |
| Negative | 8.00 | 0.60 | 13.42 | 1.03 | t(11) = -5.03, $p <$ .001 |
| Excitement | 5.50 | 0.38 | 6.92 | 0.57 | t(11) = -2.83, $p$ = .016 |
| Cognitive | 5.50 | 0.29 | 10.25 | 0.72 | t(11) = -6.71, $p <$ .001 |
| Positive | 4.08 | 0.08 | 6.92 | 0.48 | t(11) = -6.19, $p <$ .001 |
| Depression | 5.67 | 0.23 | 10.17 | 0.44 | t(11) = -9.95, $p <$ .001 |
| Disorganisation | 3.08 | 0.08 | 5.50 | 0.65 | t(11) = -4.05, $p$ = .002 |
| Total | 35.83 | 1.00 | 58.58 | 2.43 | t(11) = -11.10, $p <$ .001 |

**Table S2**. Labels from the Harvard-Oxford cortical and subcortical structural atlases. Side (R = right; L = left), MNI coordinates (X, Y, Z) and *t*-values of the anatomical regions showing statistically significant differences between the placebo and ketamine conditions. All these regions showed a bigger *gamma-band* (30-90 Hz) power in the ketamine compared to the placebo condition.

| Label | Side | X | Y | Z | *t*-value |
|---|---|---|---|---|---|
| Hippocampus | R | 10 | -10 | -20 | 7.81 |
| Thalamus | R | 10 | -20 | 10 | 6.89 |
| Thalamus | L | -10 | -20 | 10 | 6.67 |
| Fusiform | L | -40 | -10 | -30 | 5.7 |
| Medio frontal cortex | R | 0 | 40 | -20 | 5.22 |
| Frontal pole | L | -20 | 40 | -10 | 4.91 |
| Superior Frontal Gyrus | L | -20 | 40 | 40 | 4.11 |
| Superior Temporal Gyrus | L | -70 | -20 | 0 | 3.48 |
| Middle Temporal Gyrus | L | -60 | 0 | -30 | 2.77 |

**Table S3.** Labels from the Harvard-Oxford cortical and subcortical structural atlases. Side (R = right; L = left), MNI coordinates (X, Y, Z) and *t*-values of the anatomical regions showing statistically significant differences between the placebo and ketamine conditions. All these regions showed a reduced *beta-band* (13-30 Hz) power in the ketamine compared to the placebo condition.

| Label | Side | X | Y | Z | *t*-value |
|---|---|---|---|---|---|
| Cerebellum | | 0 | -40 | -20 | -5.44 |
| Precuneus | L | -20 | -50 | 20 | -5.38 |
| Precuneus | R | 30 | -50 | 10 | -4.68 |
| Middle Temporal Gyrus | R | 60 | -30 | -10 | -3.88 |
| Anterior Cingulate | L | 0 | 30 | -10 | -3.83 |
| Inferior Tempoal Gyrus | R | 50 | -60 | -20 | -3.6 |
| Visual cortex | R | 30 | -90 | -10 | -2.89 |

## Supplementary Methods

*Psychiatric screening*

1. Structured Clinical Interview for DSM-IV (SCID-II) (First, Gibbon, Spitzer, Williams, & Benjamin, 1997).
2. Schizotypal Personality Questionnaire SPQ-G (Raine, 1991).
3. Symptom Checklist 90 (SCL90) (Derogatis, Lipman, & Covi, 1973).

*Psychological assessment*

1. Brief Assessment of Cognition in Schizophrenia battery (BACS) (Keefe et al., 2004).
2. Edinburgh Handedness Inventory (EHI) (Oldfield, 1971).
3. Verbal intelligence test (Lehrl, 1989).

*MEG analysis – Beamforming*

Power-spectra were source-localized using a beamformer technique in the frequency domain with a Dynamical Imaging of Coherent Sources (DICS) beamformer (Gross, 2001). The estimation of source power at each voxel was performed by a spatially adaptive filter that was divided into a regular 10 mm 3D dipole grid (see supplementary info for more details). To calculate the forward model, a realistic volume conductor model (Nolte, 2003) was used and the individual head shapes were aligned to the MEG data by means of fiducial markers. Finally, the covariance matrix for each individual was computed with a multi-taper Fast-Fourier transformation and source power was calculated for each grid point.

*MEG analysis – Labeling clusters of activity*

The source-level cluster-based analysis highlighted clusters of voxels showing increased gamma and decreased beta band activity after ketamine administration. T-metrics, as generated by the cluster based corrected paired t-test (see source-level analysis in the main manuscript) were used to identify "local extrema" within each cluster. Local extrema were localized by considering the voxel with the most extreme (most positive for the gamma statistics or negative for the beta statistics) *t*-value than the 26 neighboring voxels. As such, we can be confident that the identified extrema are not extensions of other clusters. The anatomical label of local maxima has then been localized using the Harvard-Oxford cortical atlas and the Harvard-Oxford subcortical atlas.

*MEG analysis -Transfer entropy*

To investigate the effects of ketamine on the interactions between sources, we quantified changes in information transfer by measuring transfer entropy (TE) functional (Schreiber, 2000). TE is a model free analysis of functional interactions which measures the amount of information from a source arriving at a target that is not contained in the targets history, or that can only be decoded together with the targets history (Wibral et al., 2013; Wibral, Vicente, & Lindner, 2014). We used the TE estimation algorithms implemented in the TRENTOOL toolbox (Lindner, Vicente, Priesemann, & Wibral, 2011; Wollstadt, Martinez-Zarzuela, Vicente, Diaz-Pernas, & Wibral, in press).

The TE functional is a specific conditional mutual information *I(. : . | . )* between an information source X and a target of the information transfer Y: TE(X->Y, δ) = I(Y(t) : **X**(t-δ) | **Y**(t-1)), where Y(t) is the current sample of the target time series, and where **X**(t- δ), **Y**(t-1) are past states of source and target time series, respectively (Lindner et al., 2011; Vicente, Wibral, Lindner, & Pipa, 2011) and δ is the physical delay of the interaction between source and target. This delay can be found via an optimization procedure described in Wibral et al.

(Wibral et al., 2013) as: $\delta = \text{argmax}_u \text{TE}(X->Y, u)$, where u is an assumed delay that is scanned for a range of values until a maximal TE value is found. Here, TE was computed for assumed physical delays *u* between 4 and 30 ms and the value at the maximal TE was chosen for each link, participant and condition.

Time courses for the TE analysis were reconstructed from the anatomical regions showing a statistically significant drug effect (ketamine vs. placebo). Raw data was first filtered with a 10 to 150 Hz bandpass, followed by a time-domain linear constrained minimum variance (LCMV) beamformer (Van Veen, van Drongelen, Yuchtman, & Suzuki, 1997), which enabled the reconstruction of source time courses for three orthogonal dipoles in the cardinal directions.

On these three time courses, a principal component analysis was performed in order to determine the dominant dipole orientation (i.e., direction with the largest variance), which was used for subsequent TE computation. The state space embedding dimension was allowed to a range from 2 to 10, and was optimized jointly with the embedding lag parameter $\tau$ using the Ragwitz criterion (Ragwitz & Kantz, 2002) for each participant. Since differing embedding dimensions can bias TE results (Kraskov, Stogbauer, & Grassberger, 2004), while a slight over-embedding does not compromise the detection of significant TE (Lindner et al., 2011), the TE group comparison between the ketamine and placebo conditions was carried out considering the maximal embedding dimension of $d = 5$ across all conditions and participants.

A kernel-based estimator (Kraskov et al., 2004) was used with a fixed mass search for next neighbors (n = 4) in the joint space. Faes' method was implemented to remove residual volume conduction effects (Faes, Nollo, & Porta, 2013). Finally, a graph algorithm separated direct from indirect interactions by identifying alternative paths with similar sums of delay times (Wollstadt et al., in press). Thus, spurious effects due to cascades could be detected and

removed.

In the first step, we assessed global change in TE between all sources at beta/gamma-frequencies which were characterized by significant modulation through ketamine through averaging TE values across all links per participant and conditions. To localize the links, a one-sided permutation test for each link was performed and the alpha level was corrected for multiple comparison. Given the number of sources (n = 16) and the number of potential interactions for each source (n = 15), *p* was set to 0.05 / 240 (2.08 * 10). In addition, we investigated TE-changes separately for interactions between sources in the beta- and gamma-frequency ranges as well as between the two spectral bands. The alpha level was set to $2.08 * 10^{-4}$.

## References

Derogatis, L. R., Lipman, R. S., & Covi, L. (1973). SCL-90: an outpatient psychiatric rating scale - preliminary report. *Psychoparmacological Bulletin, 9*, 13-28.

Faes, L., Nollo, A., & Porta, A. (2013). Compensated transfer entropy as a tool for reliably estimating information transfer in physiological time series. *Entropy, 15*(1), 198-219.

First, M. B., Gibbon, M., Spitzer, R. L., Williams, J. B. W., & Benjamin, L. S. (1997). Structured Clinical Interview for DSM-IV Axis II Personality Disorders, (SCID-II). *Washington, D.C.: American Psychiatric Press, Inc., 1997.*

Gross, J. (2001). Dynamic imaging of coherent sources: Studying neural interactions in the human brain. *Proceedings of the National Academy of Sciences, 98*, 694-699.

Keefe, R. S., Goldberg, T. E., Harvey, P. D., Gold, J. M., Poe, M. P., & Coughenour, L. (2004). The Brief Assessment of Cognition in Schizophrenia: reliability, sensitivity, and comparison with a standard neurocognitive battery. *Schizophr Res, 68*(2-3), 283-297. doi: 10.1016/j.schres.2003.09.011

Kraskov, A., Stogbauer, H., & Grassberger, P. (2004). Estimating mutual information. *Phys Rev E Stat Nonlin Soft Matter Phys, 69*(6 Pt 2), 066138.

Lehrl, S. (1989). Mehrfachwahl-Wortschatz-Intelligenztest: MWT-B / Siegfried Lehrl.2. überarbeitete Auflage. *Perimed-Fachbuch-Verl.-Ges., Erlangen*.

Lindner, M., Vicente, R., Priesemann, V., & Wibral, M. (2011). TRENTOOL: A Matlab open source toolbox to analyse information flow in time series data with transfer entropy. *BMC Neurosci, 18*, 12:119.

Nolte, G. (2003). The magnetic field theorem in the quasi-static approximation and its use for magnetoenchephalography forward calculation in realistic volume conductors. *Physics in Medicine and Biology, 48*(22), 3637-3652.

Oldfield, R. C. (1971). The assessment and analysis of handedness: The Edinburgh inventory. *Neuropsychologia, 9*, 97-113.

Ragwitz, M., & Kantz, H. (2002). Markov models from data by simple nonlinear time series predictors in delay embedding spaces. *Phys Rev E Stat Nonlin Soft Matter Phys, 65*(5 Pt 2), 056201.

Raine, A. (1991). The SPQ: A Scale for the Assessment of Schizotypal Personality Based on DSM-III-R Criteria *Schizophr Bull, 17*(4), 555-564.

Schreiber, T. (2000). Measuring information transfer. *Physics reviews Letters, 85*, 461-464.

Van Veen, B. D., van Drongelen, W., Yuchtman, M., & Suzuki, A. (1997). Localization of brain electrical activity via linearly constrained minimum variance spatial filtering. *IEEE Transactions of Biomedical Engeneering, 44*(9), 867-880.

Vicente, R., Wibral, M., Lindner, M., & Pipa, G. (2011). Transfer entropy--a model-free measure of effective connectivity for the neurosciences. *J Comput Neurosci, 30*(1), 45-67. doi: 10.1007/s10827-010-0262-3

Wibral, M., Pampu, N., Priesemann, V., Siebenhühner, F., Seiwert, H., Linder, M., . . . Vicente, R. (2013). Measuring information-transfer delays. *PLoS ONE, 8*(2), e55809.

Wibral, M., Vicente, R., & Lindner, M. (2014). Transfer Entropy in Neuroscience. In Springer (Ed.), *Directed Information Measures in Neuroscience*. Berlin Heidelberg: Springer.

Wollstadt, P., Martinez-Zarzuela, M., Vicente, R., Diaz-Pernas, F., & Wibral, M. (in press). Efficient transfer entropy analysis of non-stationary neural time series. *PLoS ONE*.